Review Article

Investig Clin Urol 2022;63:385-393.
https://doi.org/10.4111/icu.20220059
pISSN 2466-0493 • eISSN 2466-054X

INVESTIGATIVE AND CLINICAL UROLOGY
ICUROLOGY

Understanding cavitation-related mechanism of therapeutic ultrasound in the field of urology: Part I of therapeutic ultrasound in urology

Sung Yong Cho[1,*], Ohbin Kwon[2,*], Seong-Chan Kim[2], Hyunjae Song[3], Kanghae Kim[2], Min Joo Choi[2,4]

[1]Department of Urology, Seoul National University Hospital, Seoul National University College of Medicine, Seoul, [2]Interdisciplinary Postgraduate Program in Biomedical Engineering, Jeju National University, Jeju, [3]Department of Electronic Engineering, Sogang University, Seoul, [4]Department of Medicine, Jeju National University College of Medicine, Jeju, Korea

Shock waves are commonly used in the field of urology. They have two phases, positive and negative, and the bubble generation is roughly classified into acoustic cavitation (AC) and laser-induced cavitation (LIC). We evaluated the occurrence of cavitation, its duration, the area of interest, and the maximal diameter of the cavitation bubbles. Changes in AC occurred at 0.2 ms with the highest number of bubbles and disappeared at 0.6 ms. The bubble size was 2 mm in diameter. Changes in LIC bubbles were observed in three pulse modes. The short pulse showed an initial bubble starting at 0.005 ms, which reached its largest size at 0.4 to 0.6 ms. The long pulse showed an initial bubble starting at 0.005 ms, which reached its largest size at 0.4 ms with the formation of an additional lagena-shaped bubble at 0.6 ms. The distance mode of MOSES showed two signal peaks with the formation of two consecutive bubbles at 0.2 and 0.6 ms. The main difference in the laser beams between the long-pulse and the MOSES modes was the continuity and the peak power of the laser beam. The diameters parallel to the laser direction were 6.8, 8.6, and 9.7 mm at 1, 2, and 3 J, respectively, in the short pulse. While the cavitation bubbles rupture, ejectile force occurs in numerous directions, transmitting high enough energy to break the targets. Cavitation bubbles should be regarded as energy and the mediators of energy for stone fragmentation and tissue destruction.

Keywords: Acoustic waves; ESWL (Extracorporeal Shockwave Lithotripsy); Laser-induced shockwave lithotripsy; Lasers, solid-state; Photography

INTRODUCTION

Typically, shock waves have specific physical characteristics such as nonlinearity, high peak pressure with low tensile amplitude, and a short rise of time and duration. Shock waves have a positive phase with direct mechanical forces and a negative phase with cavitation bubbles, which subsequently rupture very quickly, generating additional waves [1].

Cavitation bubbles are traditionally associated with erosion damage [2] to ship propellers or hydraulic turbomachinery [3] and with biomedical applications [4] in lithotripsy [5] or microfluidics [6]. The most commonly used cavitation methods in liquids in the urologic field are acoustic cavitation (AC) and laser-induced cavitation (LIC). AC is a phe-

Received: 11 February, 2022 • **Revised:** 14 March, 2022 • **Accepted:** 17 March, 2022 • **Published online:** 26 May, 2022
Corresponding Author: Min Joo Choi https://orcid.org/0000-0003-4626-3706
Department of Medicine, Jeju National University College of Medicine, 102 Jejudaehak-ro, Jeju 63243, Korea
TEL: +82-64-754-3876, FAX: +82-64-702-2687, E-mail: mjchoi@jejunu.ac.kr
*These authors contributed equally to this study and should be considered co-first authors.

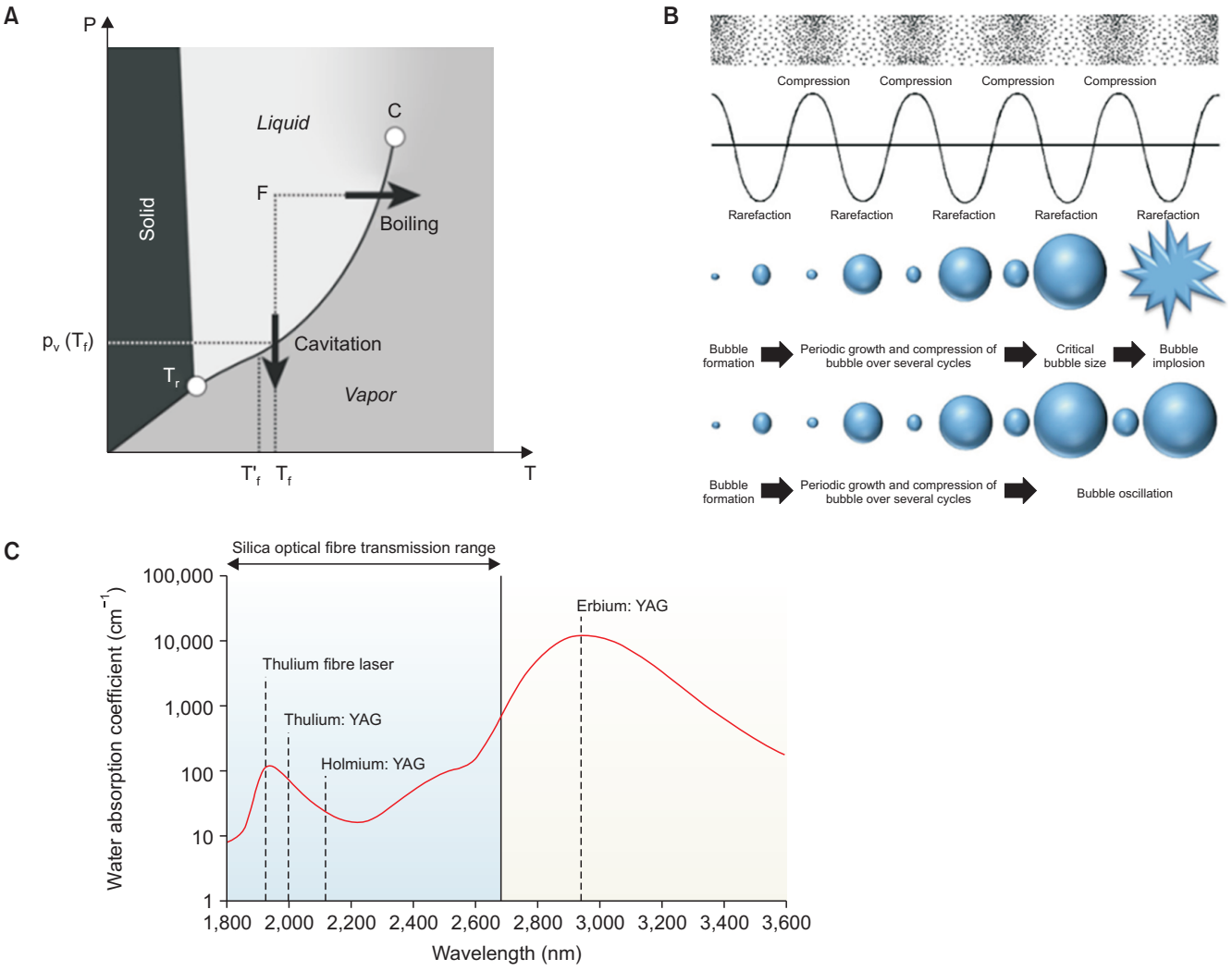

Fig. 1. (A) Formation of acoustic cavitation. The static pressure of a liquid is reduced to below its vapor pressure, leading to the formation of small vapor-filled cavities in the liquid (Revised from Franc and Michel. Fundamentals of cavitation. 2006;76 [7] with permission of Springer Nature). (B) Bubble formation, implosion, and oscillation (Revised from Izadifar et al. J Med Biol Eng 2019;39:259-76 [8] with permission of Springer Nature). (C) Water absorption coefficient of the common mid-infrared laser wavelengths including thulium and holmium lasers (Revised from Fried and Irby. Nat Rev Urol 2018;15:563-73 [9] with permission of Springer Nature).

nomenon in which the static pressure of a liquid is reduced to below its vapor pressure, leading to the formation of small vapor-filled cavities in the liquid. Second, LIC is the formation of a bubble through the decomposition of water. The bubbles are created from thermal energy generated by pulsed laser fiber light absorbed by the water medium (Fig. 1) [7-9].

When we consider biomedical applications, AC is mainly used in extracorporeal shock wave lithotripsy treatment, extracorporeal shock wave therapy, and high-intensity focused ultrasound (HIFU). LIC is primarily used in laser prostatectomy treatment, retrograde intrarenal surgery, and percutaneous nephrolithotomy. The energy transmitted by cavitation can destroy tissue, burst urinary stones [5], reduce inflammation [10], and alleviate pain [11].

1. Mechanism of the shock wave generator and the laser-induced generator

1) Shock wave generator (Rifle, HNT Medical, Seoul, Korea)

Shock waves lower the pressure below the vapor pressure of the fluid and create AC. Apart from the electrohydraulic type, electromagnetic shock wave generators employ a solenoid electromagnetic coil and use an acoustic lens or parabolic reflector to focus cylindrical or planar shock waves, respectively. The capacitor discharging voltage is level 5 of 18 kV, respectively. The positive peak pressure (P+) of the shock wave, the negative peak pressure (P-), and the energy flux density are shown in Table 1.

https://doi.org/10.4111/icu.20220059

Table 1. Maximum positive pressure (P+), maximum negative pressure (P-), and energy flux density (EFD) at the electromagnetic-type shock wave focus measured with an optical hydrophone[a]

Level	P+ (MPa)	P- (MPa)	EFD (mJ/mm^2)	Pulse length (μs)
5	27.786±0.687	-14.381±0.125	0.478±0.004	7.833±0.098

Values are presented as mean±standard deviation.
[a]:N=3. Variables measured at level 5. Optical hydrophone HPO-690 (Onda).

2) Laser-induced generator (MOSES Pulse 120H, Lumenis, Yokneam, Israel)

When laser emission occurs, the energy is absorbed into the water. As a result, it induces transient cavitation bubbles and acoustic emission around laser-heated microparticles. Cavitation bubbles are known to occur within <0.5 ns after they are heated by the laser pulse [12]. The laser power setting used for this study ranged from 0.5 to 3 J, and the maximal power of the output in the full width at half maximum is shown in Table 2.

2. Understanding pulse shaping and the occurrence of cavitation bubbles

Recently, pulse shaping has been actively used in laser treatment to modify the duration of the laser pulse or to generate complex pulses. The pulse-shaping technique was introduced as the MOSES technique or the virtual basket in the field of urology, and it can also modify the occurrence of cavitation bubbles. When cavitation bubbles are modified by MOSES technology, the second bubble goes through the first big bubble [13]. This technique is related to the formation of cavitation bubbles, which is fundamental to understanding the use of shock waves in various fields. Therefore, this study will describe how cavitation bubbles are generated by the two methods of AC and LIC and the similarities and the differences in the physical characteristics as part I of therapeutic ultrasound in urology. The characteristics of the cavitation bubbles modified by pulse shaping are described in other sections.

HOW TO MEASURE THE CAVITATION BUBBLES

1. How to measure cavitation bubbles

The properties of the shock waves and cavitation bubbles produced by the generators were evaluated by using a high-intensity broadband fiber optical hydrophone (HPO-690, Onda Corp., Sunnyvale, CA, USA), a passive cavitation detector (PCD, PA1263, Precision Acoustics Ltd, Dorchester, UK),

Table 2. Measured power (W) with the photodetector using the laser power setting[a]

Mode	Pmax (W)	FWHM (μs)	Laser pulse integral (x1e-3)
Short	12.62±0.79	144.89±4.26	1.73±0.12
Long	5.00±0.29	506.97±15.91	1.81±0.09
MOSES (distance)			
1st pulse	13.11±1.73	48.56±4.70	1.77±0.07
2nd pulse	10.62±1.02	121.83±15.02	

Values are presented as mean±standard deviation.
FWHM, full width at half maximum.
[a]:N=10. Photodetector PDA10D2 (Thorlabs).

a high-speed camera (VEO710, Vision Research, Wayne, NJ, USA), and a photodetector (PDA10D2, Thorlabs, Newton, NJ, USA). The optical hydrophone measured the acoustic pressure of AC and LIC, whereas the PCD with 4.6- and 0.5-MHz transducers evaluated the time-dependent changes in wave-patterned laser power and the pressure of the cavitation bubbles at the highest point of pressure (P+) with different AC and LIC sensors (Fig. 2). We evaluated the acoustic pressure induced by the laser from a distance, the distance at which the laser would not break the sensor. In addition, we acquired lateral images of the water tank with a high-speed camera (VEO710, Vision Research) to capture the dynamic features of the cavitation bubbles and the tip of the laser fiber. The camera captures at a rate of 7,500 images per second in full format and 200,000 images at a resolution of 128×128 pixels (128×64 pixels at 360,000 images). We evaluated the occurrence of cavitation, the duration, the area of interest, and the maximal diameter of the cavitation bubbles.

2. Acquisition of phantom gel pictures

Pictures of the phantom gel and the resulting gel damage induced by the cavitation bubbles were taken after shock wave transmission by use of an EOS 5D Mark III DSLR camera (Canon, Tokyo, Japan).

THE CHANGES IN CAVITATION BUBBLES

1. Characteristics of cavitation bubbles

The changes in cavitation bubbles induced by AC are shown in Fig. 3. The bubbles occurred in greatest number at around 166 μs (time to reach the focus of the shockwave) and disappeared at about 0.6 ms. The bubbles were approximately 2 mm in diameter. A higher number of cavitation bubbles was seen at the higher energy setting of the generator (data not shown). The hydrophone signal shown as a red line in Fig. 3 indicates the initial pressure peak and the first

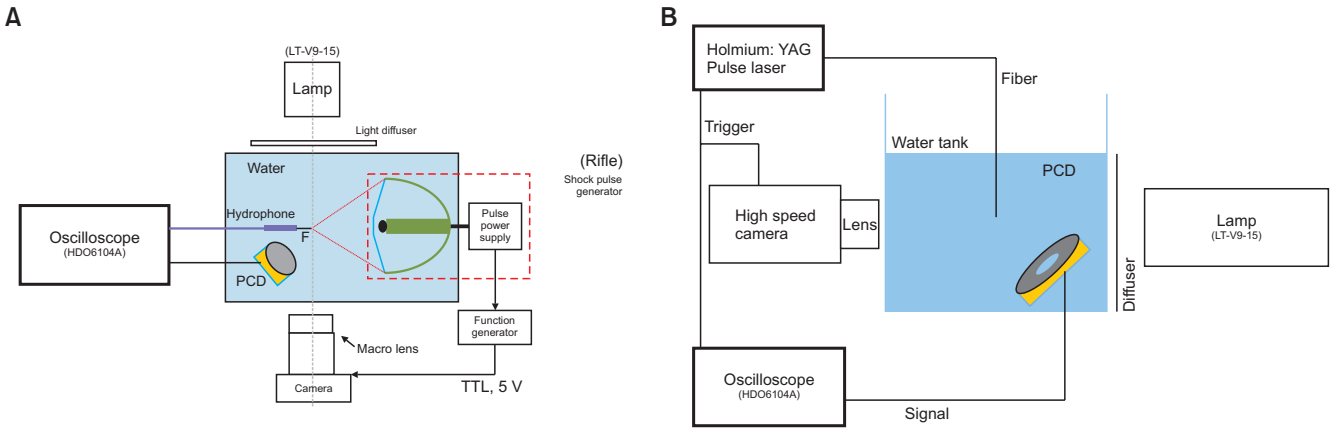

Fig. 2. Schematic block diagram of the experimental setup. (A) Acoustic cavitation generator. (B) Laser-induced cavitation generator. LT-V9-15 (GsVitec, Bad Soden-Salmünster, Germany), HDO6104A (LeCroy, New York, NY, USA), Rifle (HNT Medical, Seoul, Korea). PCD, passive cavitation detector; TTL, transistor-transistor logic.

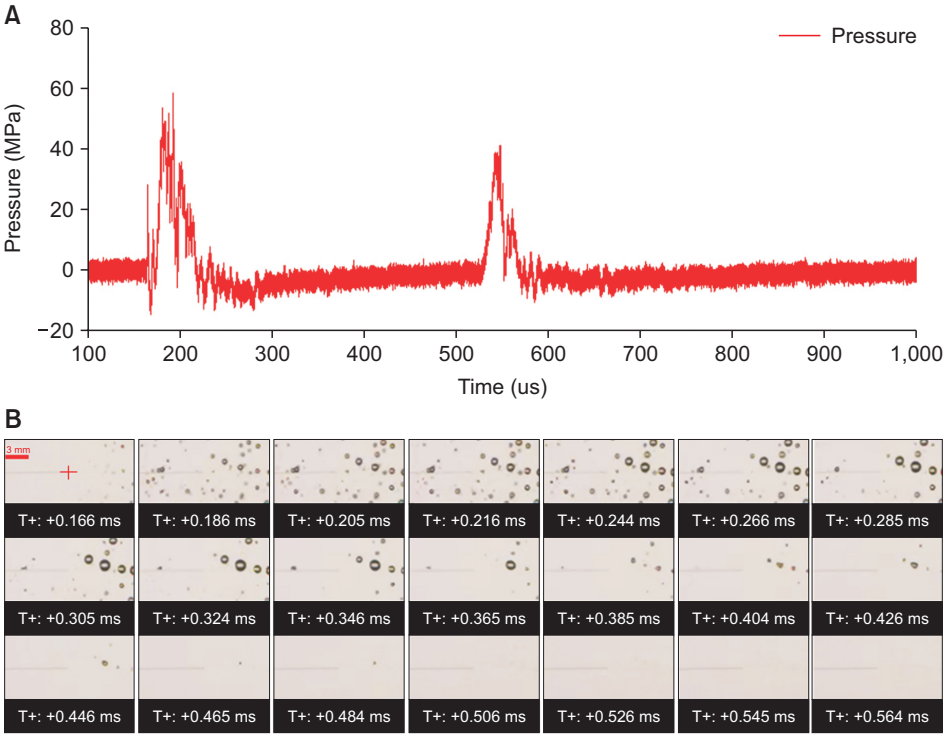

Fig. 3. (A) Signals of acoustic pressure and cavitation collapse measured at the beam focus of the shock wave generator. (B) Time-dependent variation of acoustic bubbles according to the shock wave generator setting with the 360,000 FPS and the shock wave acoustic pressure. Note: At level 5 (capacitor discharging voltage: 18 kV), the cross mark in the center of the first image is the tip of the optical hydrophone tip located at the focal point. T+, from trigger.

collapse period. The big bubbles started to rupture at around 0.2 ms and multiple second peaks of pressure were seen at about 0.6 ms, indicating the second collapse period of the big and small bubbles. The PCD signal shown by the blue line just before 0.4 ms in Fig. 3 shows the voltage change in the second peak due to the collapse of the big bubbles. Multiple cavitation bubbles occurred right after shock wave transmission, as shown in Fig. 4. The ejective force generated by numerous bubbles can destroy targets such as urinary calculi, prostate muscle, and vascular structures.

The changes in LIC bubbles are shown in Fig. 5. (1) The high-speed camera detected an initial bubble starting at about 0.005 ms and becoming largest at about 0.4 to 0.6 ms at an energy of 2 J in the short-pulse mode. The photodetector recognized the first peak (red line) of the laser beam power, and the PCD signals measured the voltage change indicating the collapse of the first big bubble and several consecutive small bubbles. (2) The long pulse showed the initial bubble starting at about 0.005 ms and becoming the largest at about 0.4 ms with continuous laser emission and the formation of an additional lagena-shaped bubble at about 0.6 ms. This lagena-shaped bubble was oriented toward the direction of the laser. The intensity of the bubble was highest before visible bubbles started to expand in size and was

https://doi.org/10.4111/icu.20220059

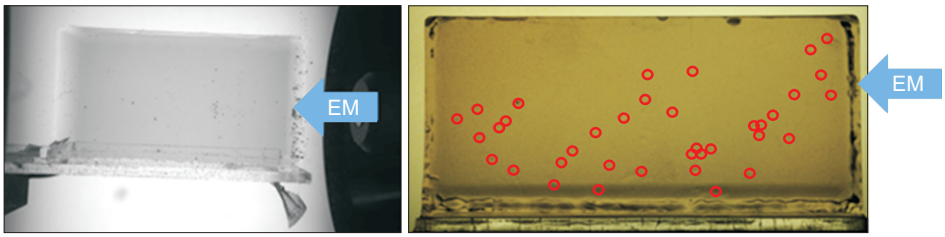

Fig. 4. Phantom gel damage induced by the cavitation bubbles generated by the shock wave generator. EM, electromagnetic shock wave generator.

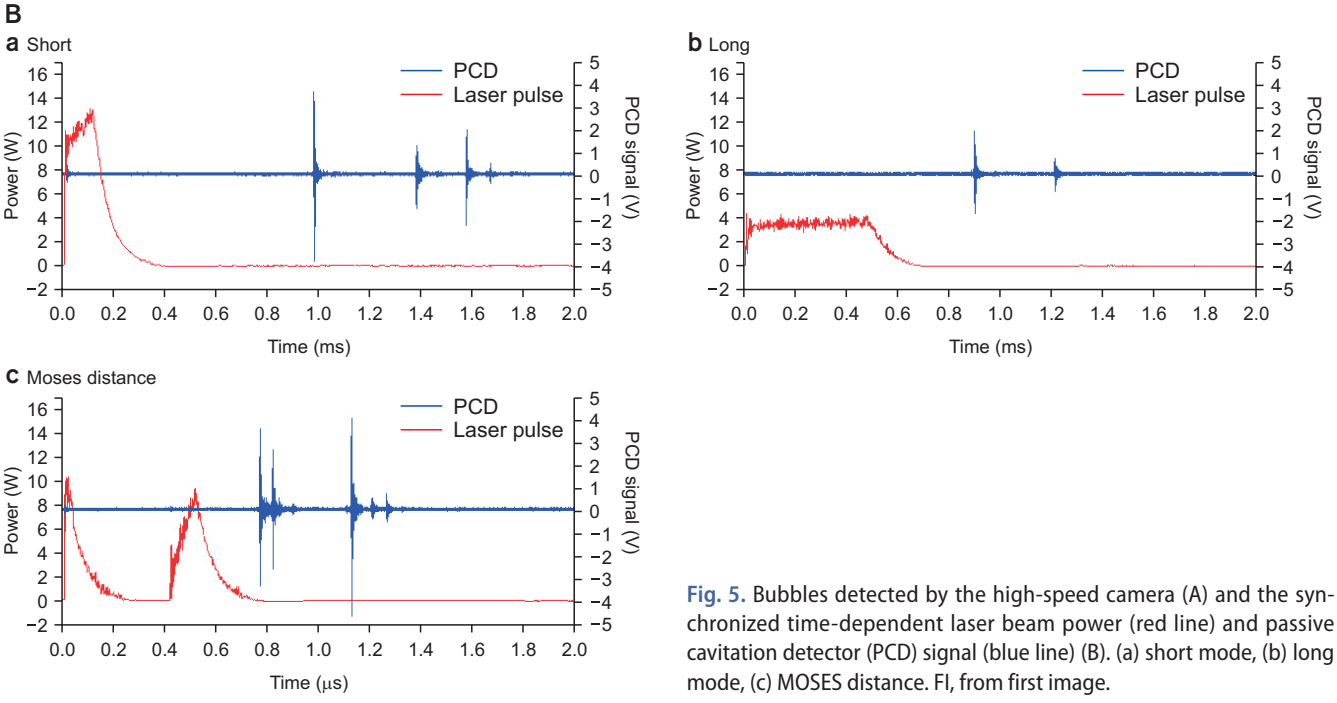

Fig. 5. Bubbles detected by the high-speed camera (A) and the synchronized time-dependent laser beam power (red line) and passive cavitation detector (PCD) signal (blue line) (B). (a) short mode, (b) long mode, (c) MOSES distance. FI, from first image.

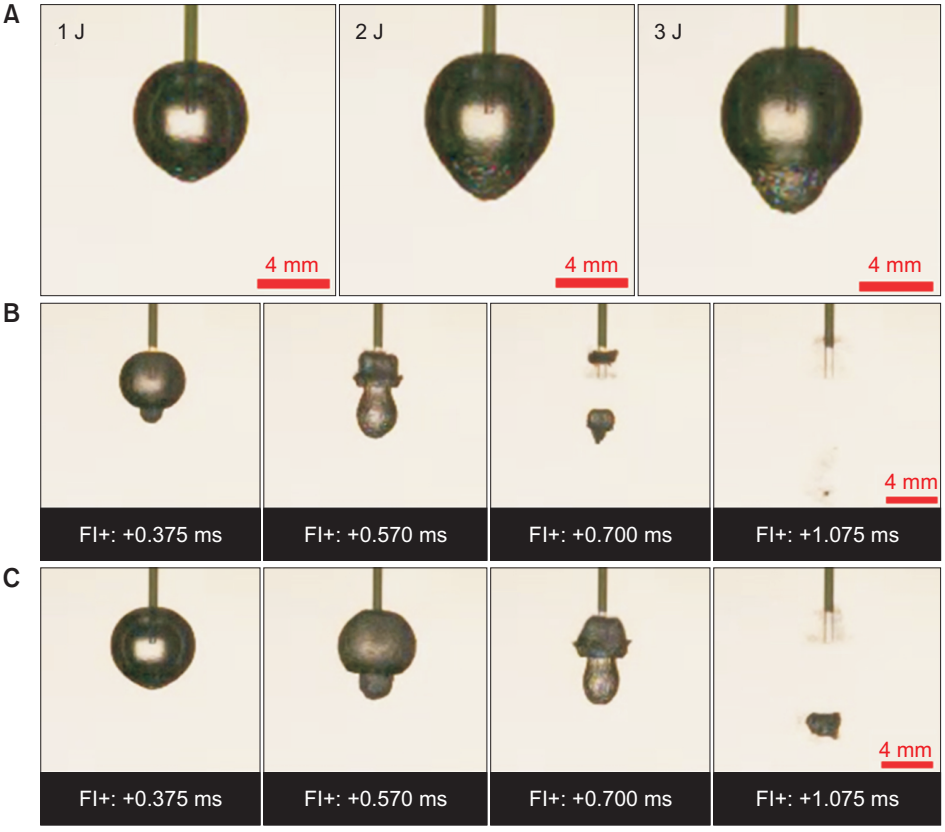

Fig. 6. (A) Differences in laser-induced cavitation bubble size according to a laser setting of 200,000 FPS. Formation of cavitation bubbles using MOSES technology in the contact mode (B) and distance mode (C). FI, from first image.

maintained for 0.3 to 0.4 ms, after which the intensity started to decrease at about 0.6 ms. Then, the initial big bubble started to rupture. The PCD noted the voltage change when the rupture of the bubbles occurred at about 0.9 and 1.2 ms. Additional changes in voltage and pressure were detected when the small bubbles started to expand and rupture at the same time right after the rupture of the first big bubble. (3) The distance mode of MOSES showed two photodetector signal peaks from the formation of two consecutive bubbles at about 0.2 and 0.6 ms. The main difference between the laser beam long-pulse and the MOSES modes at 0.2 and 0.6 ms was the continuity and the peak power of the laser beam. The interrupted laser beam of the MOSES mode generated a high peak power and the multiple, separated groups of bubbles ruptured at approximately 0.8 and 1.1 ms.

2. Pulse shaping and cavitation bubbles

The size of LIC bubbles can differ according to the laser power, as shown in Fig. 6. The longitudinal diameters parallel to the laser direction were about 6.8, 8.6, and 9.7 mm at laser powers of 1, 2, and 3 J, respectively. When the MOSES contact and distance modes were compared, the initial bubbles were maintained for about 0.650 and 800 ms, respectively. The pulse-shaped second bubble started to eject through the initial big bubble in the direction of the laser at approximately 0.330 to 0.500 ms and disappeared at about 1.0 to 1.2 ms. These findings indicate that the total maintenance time of the initial big bubbles can differ. The initial big bubble was largest in the short-pulse mode and smallest in the MOSES mode, although the total transmitted energy was the same.

DISCUSSION

1. What are the differences between the bubbles in acoustic cavitation and laser-induced cavitation?

Cavitation is the key information fundamental to understanding the treatment mechanisms of therapeutic ultrasound in various urologic disorders, including benign prostatic hyperplasia, prostate cancer, kidney tumor, erectile dysfunction, and urinary calculi. Here we attempted to show how cavitation bubbles are generated in the AC and LIC techniques. Both methods had similarities in energy transmission in water, the subsequent bubble formation, and the mechanism of the ejective force in destroying the targets when the bubbles ruptured. Both methods showed random waterjet ejection energies when the bubbles ruptured.

However, differences were observed between AC and LIC, such as the number of cavitation bubbles, their direc-

https://doi.org/10.4111/icu.20220059

tionality, the size and shape of the bubbles, and the effect on the targets. AC is based on the change of liquid pressure to vapor pressure, and LIC is based on the decomposition of water by energy transmitted from the laser. AC can be accelerated by cavitation seeds of dissolved gas nuclei, whereas LIC cannot. When used in lithotripsy, AC does not produce substantial changes in temperature. When AC bubbles rupture violently, physical effects such as shock wave emissions, microjets, turbulence formation, and shear forces may be generated in the water. However, LIC generates a substantial amount of heat, and the target-oriented photothermal ablation seems to have a pivotal role in breaking urinary stones and destroying human tissue.

2. Cavitation bubbles in acoustic cavitation

Our findings demonstrated that AC bubbles occurred about 30 μs after shock wave transmission and disappeared in about 0.6 ms. The shape of the bubbles was almost round, and the waterjet could be found when the bubbles ruptured. The size of the bubbles was about 2 mm, and numerous bubbles were found within the focal zone. The shock waves in extracorporeal shock wave lithotripsy carry energy with changes in water pressure and create numerous AC bubbles simultaneously. Because the shock waves are focused on a target by the semi-ellipsoid reflector in the electrohydraulic machine or the acoustic lens or parabolic reflector in the electromagnetic machine, the change in pressure increases around the target in the water. While the cavitation bubbles rupture, an ejectile force is exerted in numerous directions, and this transmits energy high enough to disrupt urinary stones. Although we still do not know the proportion of pressure change or the sum of the ejectile forces for efficient stone fragmentation, cavitation bubbles are regarded as energy and the mediators of energy for stone fragmentation.

A single shock wave normally transmits destructive energy from cavitation bubbles for about 0.6 ms, and the numerous bubbles generated consequently destroy the targets. The PCD signal at about 0.4 ms in this study showed a voltage change in the second peak by the collapse of the big bubbles. Although the high-speed camera showed the rupture of the big bubbles at about 0.6 ms, the PCD voltage change at this time was minimal. This finding might be due to the signal cancellation effect because of the random direction of the AC, and it is possible that the temporal overlap of the cavitation bubbles could minimize the effect on the targets. Theoretically, 1,666 (1 s/0.6 ms) shock waves can be transmitted to the target without overlapping the cavitation bubbles. However, previous studies showed the superior efficacy of delivering 60 shock waves per minute compared with 90 or 120 shock waves per minute. Therefore, the effect on the target can be affected by many factors, including the electrical charging time of the generator, the direction of the ejective force during bubble rupture, and overlapping of the cavitation bubbles.

3. Cavitation bubbles in laser-induced cavitation

The shock waves induced by laser emission were maintained for about 1.1 to 1.2 ms, and repetitive laser emissions generated multiple LIC bubbles. The pulse-repetition frequency of the Ho:YAG laser used in clinical practice for stone fragmentation ranges from 10 to 80 Hz, and the frequency of the thulium fiber laser extends to several thousand Hz. The bubbles seem to be helpful in breaking the stones by producing ejectile forces, and several previous investigations showed that cavitation plays a pivotal role in stone dusting and energy delivery [13,14]. Still, we do not know the role of photothermal ablation and the sum of the ejectile forces of LIC bubbles, and further investigation is needed to clarify this.

LIC bubbles normally occur 0.005 ms after laser emission and expand in size until about 0.6 ms. They usually rupture at about 0.8 to 1.0 ms for the first time according to the pulse shape and the laser transmission. We found lagena-shaped bubbles, the maximal size of which reached 9 mm. A single bubble could be formed by a single laser emission. Pulse-shaping technology demonstrates higher efficacy of stone fragmentation with less retropulsion and better targeting than the conventional single mode of short- or long-pulse duration [15], and better destruction of the targets can be expected. Further investigations of pulse formation, modulation of the maximal pulse power, and irrigation control techniques are necessary to enhance the surgical outcomes of patients undergoing stone fragmentation.

4. Clinical meaning of the cavitation bubbles in the field of urology

When we understand how therapeutic ultrasound works in lithotripsy, we can recognize the similarities and differences across the treatment modalities used in other urology fields such as HIFU, low-intensity shock wave therapy (LISWT), and ultrasound lithotripsy used in endoscopic procedures.

(1) The mechanism of HIFU devices is referred to as *ultrasonic ablation*, and it mostly relies on ultrasonic heating under continuous or long-pulse irradiation [16]. A piezoelectric transducer is used as the HIFU source, and a transducer or lens in front of a transducer focuses the energy onto the target [17].

(2) Because it improves angiogenesis by inducing microtrauma with repetitive shear stress on penile tissue, LISWT is being applied to treat erectile dysfunction [18,19]. Although the impulsive wave of LISWT is often referred to as a shock wave and the acoustic property differs from the shock waves in lithotripsy, cavitation bubbles are produced by an impulse wave from a metallic shock wave transmitter [20]. The main difference between the shock waves of LISWT and focused ultrasound in the area of lithotripsy is that acoustic fields are seen just in front of the shock wave transmitter with a diameter of 15 mm, and the energy can be used on superficial layers of human tissue such as muscles beneath the skin or corporal tissues beneath penile skin.

(3) The generator used in ultrasonic lithotripsy generates electricity, which excites a piezoelectric crystal vibrating at a specific frequency, generating an acoustic wave of 23 to 25 kHz. The ultrasonic waves generated are transmitted to the stone to cause fragmentation. Because of the heat generated, this technology is being used only for percutaneous nephrolithotomy. Several devices combining constant ultrasonic energy with ballistic shock wave energy or an electromagnetic impactor with ultrasonic energy and suction are used for large renal stones.

5. Limitations of the present study

First, this study was based on the analysis of a single-energy shock wave burst or laser emission. Numerous shock waves and the overlapping effect of AC can produce different outcomes regarding the safety of the tissue surrounding the target. Second, we could not include LIC results according to different laser settings. However, we analyzed typical findings, which are essential to understanding the basic principles of LIC.

CONCLUSIONS

According to our investigations, AC and LIC cavitation bubbles should be regarded as energy and the mediators of energy for stone fragmentation and tissue destruction in the urologic field. Although numerous shock waves and the overlapping effect of AC can produce stone fragmentation and tissue destruction, the result is acceptable in treating urinary calculi. Better destruction of the targets can be expected with the development of the pulse-shaping technology of LIC.

FUNDING

This work was supported by the Korea Medical Device Development Fund grant funded by the Korean government (the Ministry of Science and ICT, the Ministry of Trade, Industry and Energy, the Ministry of Health & Welfare, the Ministry of Food and Drug Safety) (Project Number: KMDF_PR_20200901_0010, 1711134986) (KMDF-RnD, NTIS 202011B04) and, in part, by the National Research Foundation of Korea (1711145583, 2017R1A2B3007907, 2019R1C1008339).

AUTHORS' CONTRIBUTIONS

Research conception and design: Sung Yong Cho and Min Joo Choi. Data acquisition: Sung Yong Cho, Ohbin Kwon, Seong-Chan Kim, Hyunjae Song, and Kanghae Kim. Statistical analysis: Sung Yong Cho and Ohbin Kwon. Data analysis and interpretation: Sung Yong Cho and Ohbin Kwon. Drafting of the manuscript: Sung Yong Cho, Ohbin Kwon, and Min Joo Choi. Critical revision of the manuscript: Min Joo Choi. Obtaining funding: Sung Yong Cho and Min Joo Choi. Administrative, technical, or material support: Ohbin Kwon and Seong-Chan Kim. Supervision: Sung Yong Cho and Min Joo Choi. Approval of the final manuscript: all authors.

REFERENCES

1. van der Worp H, van den Akker-Scheek I, van Schie H, Zwerver J. ESWT for tendinopathy: technology and clinical implications. Knee Surg Sports Traumatol Arthrosc 2013;21:1451-8.
2. Ohl CD, Kurz T, Geisler R, Lindau O, Lauterborn W. Bubble dynamics, shock waves and sonoluminescence. Philos Trans A Math Phys Eng Sci 1999;357:269-94.
3. Pereira F, Avellan F, Dupont P. Prediction of cavitation erosion: an energy approach. J Fluids Eng 1998;120:719-27.
4. Brennen CE. Cavitation in medicine. Interface Focus 2015;5:20150022.
5. Coleman AJ, Choi MJ, Saunders JE, Leighton TG. Acoustic emission and sonoluminescence due to cavitation at the beam focus of an electrohydraulic shock wave lithotripter. Ultrasound Med Biol 1992;18:267-81.
6. Kwon O, Pahk KJ, Choi MJ. Simultaneous measurements of acoustic emission and sonochemical luminescence for monitoring ultrasonic cavitation. J Acoust Soc Am 2021;149:4477.
7. Franc JP, Michel JM. Fundamentals of cavitation. Dordrecht: Springer Science & Business Media; 2006;76. https://link.springer.com/book/10.1007/1-4020-2233-6.

https://doi.org/10.4111/icu.20220059

8. Izadifar Z, Babyn P, Chapman D. Ultrasound cavitation/microbubble detection and medical applications. J Med Biol Eng 2019;39:259-76. https://doi.org/10.1007/s40846-018-0391-0.
9. Fried NM, Irby PB. Advances in laser technology and fibre-optic delivery systems in lithotripsy. Nat Rev Urol 2018;15:563-73.
10. Erroi D, Sigona M, Suarez T, Trischitta D, Pavan A, Vulpiani MC, et al. Conservative treatment for Insertional Achilles Tendinopathy: platelet-rich plasma and focused shock waves. A retrospective study. Muscles Ligaments Tendons J 2017;7:98-106.
11. Farr S, Sevelda F, Mader P, Graf A, Petje G, Sabeti-Aschraf M. Extracorporeal shockwave therapy in calcifying tendinitis of the shoulder. Knee Surg Sports Traumatol Arthrosc 2011;19:2085-9.
12. Chan KF, Vassar GJ, Pfefer TJ, Teichman JM, Glickman RD, Weintraub ST, et al. Holmium:YAG laser lithotripsy: a dominant photothermal ablative mechanism with chemical decomposition of urinary calculi. Lasers Surg Med 1999;25:22-37.
13. Chen J, Ho DS, Xiang G, Sankin G, Preminger GM, Lipkin ME, et al. Cavitation plays a vital role in stone dusting during short pulse Holmium: YAG laser lithotripsy. J Endourol 2021 Nov 22 [Epub]. https://doi.org/10.1089/end.2021.0526.
14. Ho DS, Scialabba D, Terry RS, Ma X, Chen J, Sankin GN, et al. The role of cavitation in energy delivery and stone damage during laser lithotripsy. J Endourol 2021;35:860-70.
15. Majdalany SE, Levin BA, Ghani KR. The efficiency of Moses Technology holmium laser for treating renal stones during flexible ureteroscopy: relationship between stone volume, time, and energy. J Endourol 2022;35(S3):S14-21.
16. Giannakou M, Drakos T, Menikou G, Evripidou N, Filippou A, Spanoudes K, et al. Magnetic resonance image-guided focused ultrasound robotic system for transrectal prostate cancer therapy. Int J Med Robot 2021;17:e2237.
17. Chopra R. Transurethral MR-HIFU for the treatment of localized prostate cancer. J Ther Ultrasound 2015;3(Suppl 1):O59.
18. Dong L, Chang D, Zhang X, Li J, Yang F, Tan K, et al. Effect of low-intensity extracorporeal shock wave on the treatment of erectile dysfunction: a systematic review and meta-analysis. Am J Mens Health 2019;13:1557988319846749.
19. Sokolakis I, Hatzichristodoulou G. Clinical studies on low intensity extracorporeal shockwave therapy for erectile dysfunction: a systematic review and meta-analysis of randomised controlled trials. Int J Impot Res 2019;31:177-94.
20. Choi MJ, Kwon O. Temporal and spectral characteristics of the impulsive waves produced by a clinical ballistic shock wave therapy device. Ultrasonics 2021;110:106238.